Multidecadal variability of the North Brazil Current and its connection to the Atlantic meridional overturning circulation

Dongxiao Zhang,[1,2] Rym Msadek,[3,4] Michael J. McPhaden,[2] and Tom Delworth[4]

Received 15 November 2010; revised 13 January 2011; accepted 28 January 2011; published 15 April 2011.

[1] The North Brazil Current (NBC) connects the North and South Atlantic and is the major pathway for the surface return flow of the Atlantic meridional overturning circulation (AMOC). Here, we calculate the NBC geostrophic transport time series based on 5 decades of observations near the western boundary off the coast of Brazil. Results reveal a multidecadal NBC variability that lags Labrador Sea deep convection by a few years. The NBC transport time series is coherent with the Atlantic Multidecadal Oscillation in sea surface temperature, which also has been widely linked to AMOC fluctuations in previous modeling studies. Our results thus suggest that the observed multidecadal NBC transport variability is a useful indicator for AMOC variations. The suggested connection between the NBC and AMOC is assessed in a 700 year control simulation of the Geophysical Fluid Dynamics Laboratory's CM2.1 coupled climate model. The model results are in agreement with observations and further demonstrate that the variability of NBC transport is a good index for tracking AMOC variations. Concerning the debate about whether a slowdown of AMOC has already occurred under global warming, the observed NBC transport time series suggests strong multidecadal variability but no significant trend.

Citation: Zhang, D., R. Msadek, M. J. McPhaden, and T. Delworth (2011), Multidecadal variability of the North Brazil Current and its connection to the Atlantic meridional overturning circulation, *J. Geophys. Res.*, *116*, C04012, doi:10.1029/2010JC006812.

1. Introduction

[2] The North Brazil Current (NBC) flowing northward in the tropical south Atlantic, is one of the strongest western boundary currents in the world ocean. Its unique location, straddling the tropical Atlantic where equatorial currents are predominantly zonal, suggests its potential role as a major component of the Atlantic meridional overturning circulation (AMOC) [*Lumpkin and Speer*, 2003] (Figure 1). Moored current measurement at 6°–11°S off the coast of Brazil clearly revealed the strong northward flow with subsurface intensification in the upper 1200 m [*Schott et al.*, 2005]. The NBC is thus some times called the North Brazil Undercurrent (NBUC), and is primarily responsible for the AMOC upper branch return flow which crosses the tropical Atlantic [e.g., *Hazeleger and Drijfhout*, 2006]. Below the NBC, the strong Deep Western Boundary Current (DWBC) carrying the North Atlantic Deep Water (NADW) southward at depths deeper than 1200 m, represents the lower branch of the AMOC to balance the northward surface flow [*Schott et al.*, 2005]. There is a much weaker northward flow (4 Sv) in the interior tropical South Atlantic thermocline, but it is part of the lower branch of the Subtropical Cell (STC) which is balanced by the southward surface Ekman current [*Zhang et al.*, 2003]. The western boundary component of the STC in the NBC is however entangled with the large-scale AMOC and contributes to the interhemispheric transport associated with the MOC [*Hazeleger and Drijfhout*, 2006].

[3] Model studies suggest that the NBC can provide an index for the AMOC surface return flow. *Chang et al.* [2008] showed that a dramatic change of NBC transport is concurrent with a significant weakening of the AMOC, both following a significantly reduced deep water formation at high latitudes in an idealized North Atlantic "water hosing" coupled model experiment. *Rabe et al.* [2008] compared the AMOC at 10°S with the NBC in the 50 year ECCO data assimilation system, and showed that, at time scales of several years or longer, the NBC variability is a good indicator of the AMOC in their model. The most significant change they observed in the simulated AMOC/NBC was a dramatic weakening from the 1950s to the late 1960s and early 1970s, and then a strengthening since then to the 1990s. Weakening of the early decades however was attributed to the model spin-up rather than to real variability [*Köhl and Stammer*, 2008]. Advanced ocean data assimilations based on differ-

[1]Joint Institute for the Study of the Atmosphere and Ocean, University of Washington, Seattle, Washington, USA.
[2]NOAA Pacific Marine Environmental Laboratory, Seattle, Washington, USA.
[3]AOS Program, Princeton University, Princeton, New Jersey, USA.
[4]NOAA Geophysical Fluid Dynamics Laboratory, Princeton, New Jersey, USA.

0148-0227/11/2010JC006812

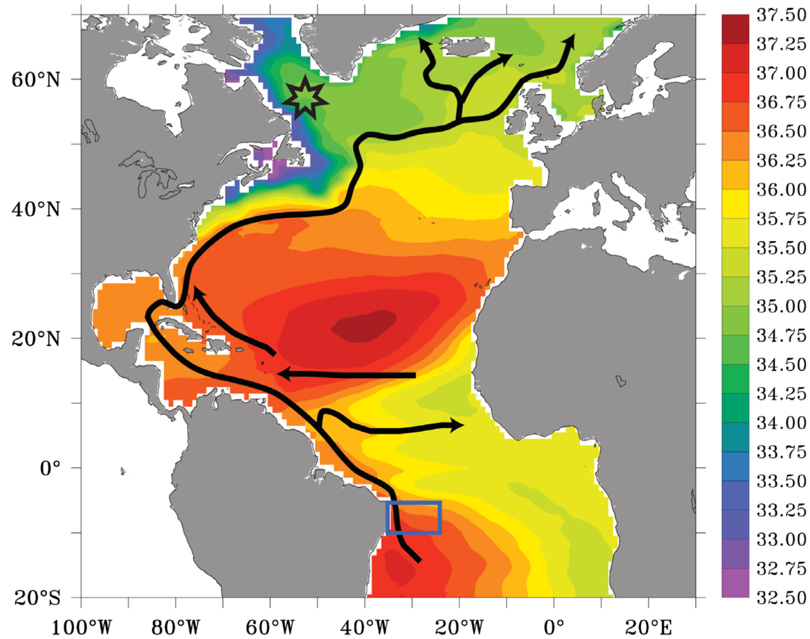

Figure 1. Schematic of upper limb of the AMOC based on *Lumpkin and Speer* [2003], superimposed on the mean salinity map at 100 m. Also shown are the Labrador Sea deep convection site (star) and the NBC region (rectangle).

ent schemes show the challenge of faithfully simulating the decadal-to-multidecadal variability of the AMOC. There appears to be no consistent low-frequency variability in AMOC transport variation in available data assimilation systems [*Schott and Brandt*, 2007; *Balmaseda et al.*, 2007; *Köhl and Stammer*, 2008]. The variations of subsurface density structure in the North Atlantic are however consistent with a gradual increasing trend of the AMOC transport from the 1970s to 2000 [*Zhang*, 2008; *Wang et al.*, 2010], in contrast to the reported weakening trend under global warming [*Bryden et al.*, 2005].

[4] The climatic impact of the NBC and its influence on Sea Surface Temperature (SST) was first discussed by *Yang* [1999] using an idealized ocean model. He showed that the NBC is the major source of AMOC variability in the tropical Atlantic, regulating the tropical Atlantic cross-hemispheric SST gradient by transporting more or less heat northward across the equator. Later, more complete coupled atmosphere-ocean general circulation models (GCMs) with several centuries long integrations suggested that multidecadal variability of the AMOC is responsible for the homogeneous basin-scale SST variability in the North Atlantic with a signature of opposite sign in the tropical South Atlantic [*Knight et al.*, 2005; *Vellinga and Wu*, 2004]. In the coupled GCM of *Vellinga and Wu*'s [2004] Figure 2, the NBC is stronger during decades of stronger AMOC composites than during weaker composites. *Chang et al.* [2008] demonstrated the potential role of NBC in abrupt climate change of the tropical Atlantic and African Monsoon during the AMOC slowdown in the Younger Dryas cold event.

[5] The primary objective of this paper is to estimate the low-frequency variability in NBC transport based on historical hydrographic observations in the western boundary of tropical South Atlantic, and to investigate the possibility of the NBC as an indicator for decadal-to-multidecadal variability of the AMOC. Data and observational results will be presented in sections 2 and 3. Two methods used for the geostrophic transport calculation will be introduced in section 2: Method 1 relies on gridded fields of the unevenly distributed temperature (T) and salinity (S) profiles in the western tropical South Atlantic with reference level of 1200 m. Method 2 directly uses profiles at onshore and offshore sides of the current without interpolation but referenced to 600 m. In section 4, a parallel analysis of a multicentury control run of the coupled climate model Geophysical Fluid Dynamics Laboratory's (GFDL's) CM2.1 [*Delworth et al.*, 2006; *Msadek et al.*, 2010] supplements the observational analysis which is limited by historical data coverage. We summarize the conclusions in section 5.

2. The Observed NBC Transport Time Series

[6] Geostrophic transports of the NBC are calculated using historical hydrographic data, obtained from the updated NOAA World Ocean Database 2009 [*Boyer et al.*, 2006]. Although data coverage in the western boundary region is much better than in the rest of the ocean, these historical data are unevenly distributed both spatially and temporally, and there is not enough data to derive yearly time series of the NBC transport. Therefore we interpolate the observed profiles to 9 year intervals on a regular grid of 0.5° latitude × 0.2° longitude using objective analysis [*Mariano and Brown*, 1992; *Zhang et al.*, 2003] in the western tropical south Atlantic, with a decorrelation scale of 5° latitude × 2° longitude. Data noise is chosen to be low in the objective analysis [*Mariano and Brown*, 1992; *Zhang et al.*, 2003] to avoid unnecessary smoothing where data are available. The resulting gridded

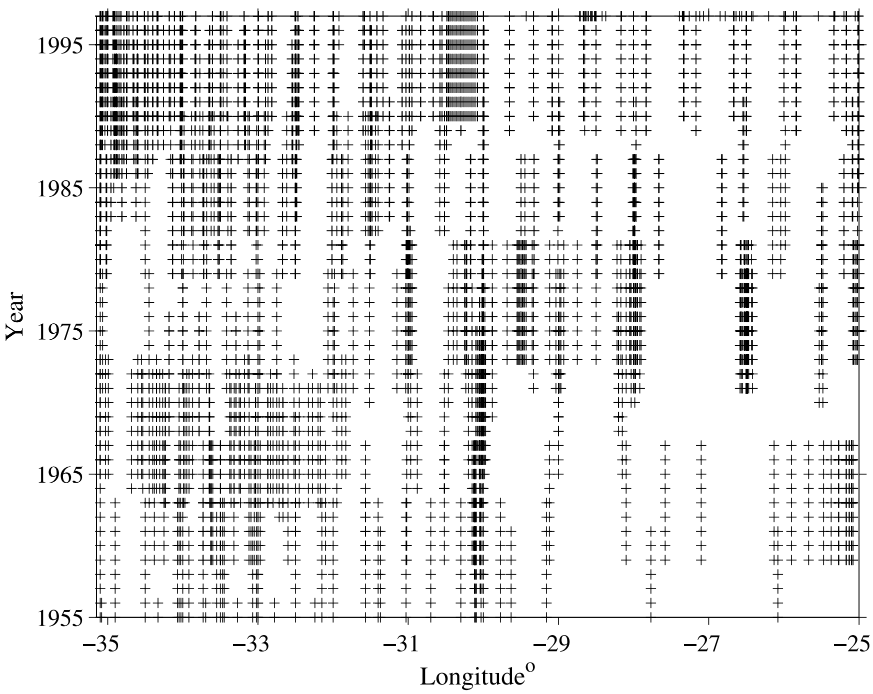

Figure 2. Data distribution of hydrocasts that had both T and S profiles reaching at least 1200 m in the region off the coast of Brazil (11.5–4.5°S, coast to 25°W).

fields correspond to the midyear of the 9 year period. This 9 year window and interpolation allows enough profiles near the coast and in the offshore side of the NBC to define the geostrophic transport of the current. The calculated transport time series from 1956 to 1996 is analogous to the 9 year running mean though our results can be aliased by short-term variations such as eddies and seasonal cycle, the effects of which shall be considered in the error analysis. Following Hydrobase [*Curry*, 1996], data and derived properties are averaged and interpolated on density surfaces. Analysis on density surfaces helps to reduce aliasing due to high-frequency vertical movement of isopycnal surfaces and artificial mixing of water masses across fronts and strong currents that is prone to occur in depth coordinate analyses [*Lozier et al.*, 1995; *Curry*, 1996; *Hazeleger and Drijfhout*, 2006]. The geostrophic calculation is referenced to 1200 m, which is the boundary between the northward NBC and the southward DWBC at 5–11°S. This reference depth has been validated using lowered acoustic Doppler current profiler (ADCP) surveys, hydrographic sections [*Schott et al.*, 2005], and the results of a model based data assimilation study [*Rabe et al.*, 2008].

[7] The zonal section from the coast of Brazil to 25°W along 6°S, where the NBC is primarily heading north, is extracted from the objective analysis for NBC transport calculations (method 1). In the gridded analysis, isopycnal surfaces are objectively mapped into the bottom topography at the coast to take into account the geostrophic shear of the boundary current over topography, following *Roemmich and McCallister* [1989] and *Bingham and Talley* [1991]. The level of no motion in the geostrophic calculation is chosen to be 1200 m or the bottom, whichever is shallower. Using method 2, we calculate the NBC transport directly using the temperature and salinity profiles at two sides of the current, since geostrophic transport only depends on the two ends of a section. It is however difficult to determine which profiles in the onshore side are to be used, because the current flows along the coast with current axis meandering between onshore and offshore positions. Since the mean NBC core is generally located east of 1200 m isobath [*Schott et al.*, 2005], here we choose to use profiles near 600 m isobath for the western side of the NBC between 4.5 and 11.5°S, the latitudinal range where the NBC transport is stable [*Schott et al.*, 2005]. We use profiles within 33–28°W for the eastern side of the NBC. Profiles in the onshore side are randomly paired to those in the offshore side for every 2° latitudinal band in each 9 year period, so that the geostrophic transport (referenced to 600 m) averaged from these pairs is equivalent to applying a 9 year running mean as in method 1.

[8] Figure 2 shows the data distribution of hydrocasts that had both temperature and salinity profiles reaching at least 1200 m in the region off the coast of Brazil (11.5–4.5°S, coast to 25°W), for every 9 years centered from 1955 to 1996. The gesotrophic transport calculation critically depends on the two ends near 35°W and 30°W that enclose the NBC and its offshore recirculation. There are about 70% more hydrocasts reaching 600 m than 1200 m in this region. Using method 2, we are able to extend the NBC transport time series derived from method 1 (1956–1996) to 1999. In recent years Argo floats begin to provide real time coverage in the open ocean, but the lack of profiles over the shelf in the western boundary prevents us from extending our transport calculation after 2000. Note however that our calculation for the last year 1999 uses all the data collected during the 9 year window between 1995 and 2003.

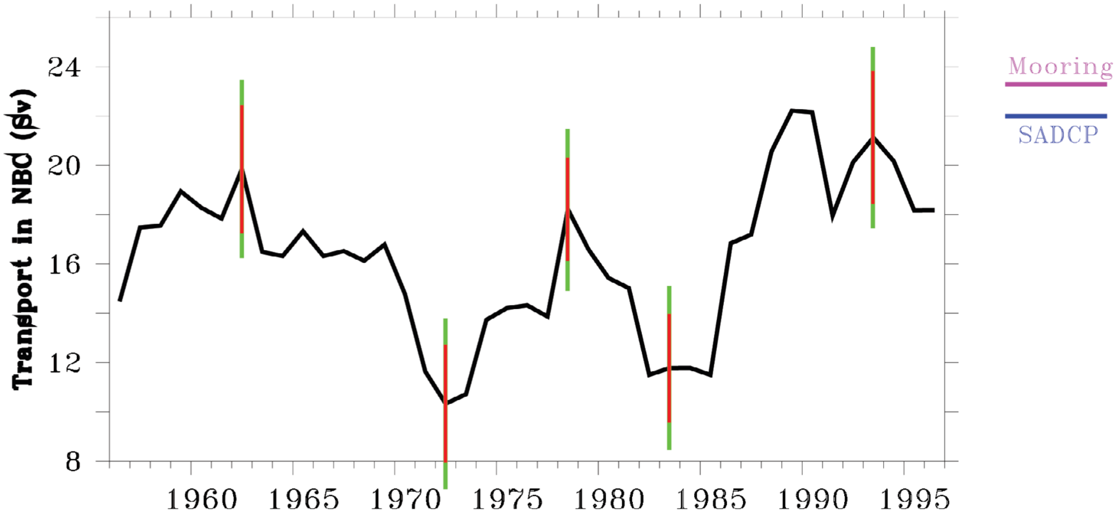

Figure 3. Time series of the NBC geostrophic transport using method 1. Green error bars of NBC transport include the potential aliasing from the seasonal cycle in addition to uncertainties due to data distribution, eddies, and offshore recirculation as indicated by red error bars. Mean transports from mooring and ship ADCP (SADCP) measurements of *Schott et al.* [2005] during 2000–2004 are shown on the right (see details in text), where the horizontal lines are positioned to show both the transport values and the time window when measurements take place.

[9] Figure 3 shows the multidecade time series of NBC transport calculated in method 1. Though the eddy related high-frequency variability is small at 6°S compared to higher latitudes, the offshore southward recirculation of the NBC could introduce large errors in transport estimates if not completely resolved [*Schott et al.*, 2005; *Zhang et al.*, 2003]. Our NBC transports are therefore integrated from the coast to several hundred kilometers offshore to ensure that the recirculation is properly accounted for. Our error bars in transport time series are conservative and include uncertainties associated with the data distribution, the extent of offshore recirculation (as with *Zhang et al.* [2003]), and aliasing of seasonal cycle. To derive error bars, we smoothed the cumulative transport curves integrated from the coast to 25°W using spline fitting and we define the errors as the largest deviations across the zonal section between the smoothed and the original cumulative transport curves. The logic behind this error estimate is that these deviations could be caused by the aliasing of incompletely resolved high-frequency and small-spatial-scale oceanic processes, including the shifts of NBC axis and its recirculation, as well as mesoscale eddies in the shipboard data. The average of these errors from longitudinal sections between 11.5 and 4.5°S in the gridded fields for selected periods are shown by the error bars (red) in Figure 3 for the NBC transport estimation at 6°S. Since there were not enough data to cover all seasons in those 9 year periods, the amplitude of the NBC seasonal cycle (2.5 Sv) [*Schott et al.*, 2005] is also included to account for possible seasonal aliasing. The combined errors are shown by the green error bars.

[10] The transport values in our time series are in agreement with lowered ADCP measurements of *Schott et al.* [2005] during an overlapping period at the end of our record. Schott et al. reported NBC transports with recirculation of 22.1 Sv (1990–2004 mean ADCP section at 5°S), 21.7 Sv (2000–2004 mean ADCP section at 11°S), and 23.3 Sv (2000–2004 mean moored currents at 11°S with partial recirculation). The latter two estimates are shown in Figure 3 for comparison with our transport time series. The decadal variability of the NBC transport can be compared to the ocean model simulations of *Hüttl and Böning* [2006], which were forced by realistic wind and heat flux variations from the NCEP/NCAR reanalysis (Figure 4a). The observed decadal variability with a standard deviation of 3.1 Sv is larger than their model results, because their NBC transports were integrated from simulated western boundary current in the upper 300 m only. Our transport integrated in the upper 300 m (Figure 4b) shows comparable variability (standard deviation of 1.7 Sv) and is about the same as the transport variability calculated by method 2 (standard deviation of 1.9 Sv) using a reference level of 600 m. The high-correlation (0.67, above 95% significance level) between the transport time series given by the two independent methods suggest that the variability was not caused by aliasing from relatively few observations in deeper levels or the interpolation of the objective analysis. The weaker transport variability in method 2 compared to method 1 also suggests a significant coherent variability of the current between 600 and 1200 m.

3. Possible Links to the AMOC

[11] Since there is no observed multidecadal AMOC transport time series to be compared with, we compare our NBC transport timeseries to the decadal variability of the Labrador Sea Water (LSW) thickness (Figure 5). The LSW formation has long been viewed as the major mechanism for NADW formation [*Curry et al.*, 1998], with additional contributions from overflows of the Nordic Seas. Modeling studies have shown that decadal variability in LSW drives

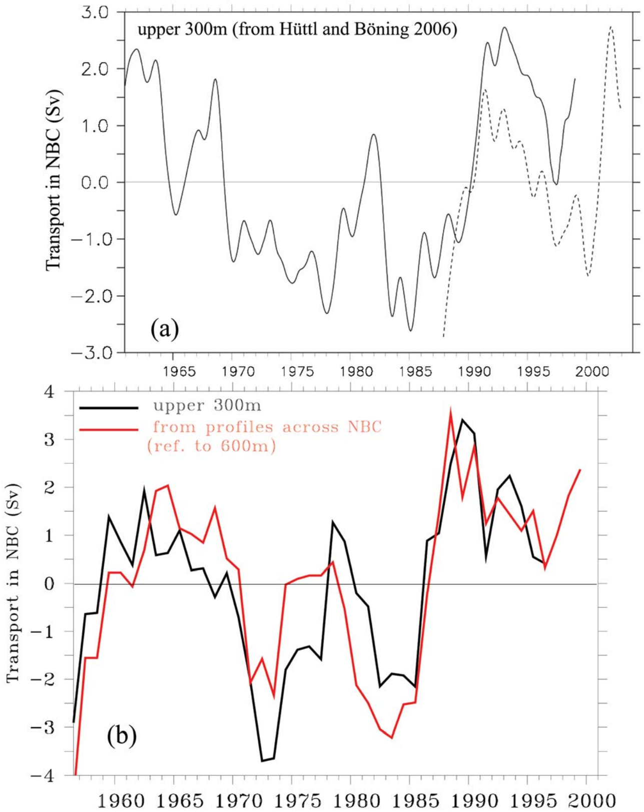

Figure 4. (a) The NBC transport anomalies (upper 300 m) in 1/3° eddy permitting (solid) and 1/12° eddy resolving (dashed) ocean simulation forced by realistic fluxes [*Hüttl and Böning*, 2006]. (b) The upper 300 m geostrophic transport in NBC (referenced to 1200 m) calculated by method 1 and geostrophic transport calculated in method 2 (referenced to 600 m). Mean transport in both time series are removed.

AMOC fluctuations in ocean models through relatively quick dynamical ocean adjustment [*Yang*, 1999; *Johnson and Marshall*, 2004; *Getzlaff et al.*, 2005; *Hüttl and Böning*, 2006]. Due to a lack of direct multidecadal measurements of AMOC strength, the LSW thickness has been used as an indicator of deep convection in the Labrador Sea and, by proxy, of AMOC variability [*Curry et al.*, 1998; *Latif et al.*, 2006]. We calculated LSW thickness from objectively mapped depths of two density surfaces, $\sigma_{1.5}$ = 34.62 and $\sigma_{1.5}$ = 34.72, as with *Curry et al.* [1998]. The objective analysis in the subpolar North Atlantic was done every 9 years, similar to our analysis in the tropical south Atlantic. The error bars of LSW thickness were derived from objective mapping errors [*Mariano and Brown*, 1992] at the center of the Labrador Sea. The highest correlation between LSW and NBC is 0.81 (above 95% significance) when LSW leads by 2 or 3 years. The 95% significant level is 0.46, based on 17 degrees of freedom as determined by the integral time scale of the time series [*Davis*, 1976]. The 2–3 year lag is in excellent agreement with the time scale of dynamic adjustment reported for eddy permitting ocean models [*Getzlaff et al.*, 2005]. They showed that the delay is much longer in their coarse resolution models that do not fully represent the relatively fast time scale dynamical adjustment that occurs along the western boundary and the boundary between the subtropical and subpolar gyres.

[12] Many studies have identified the AMOC as one driver of the Atlantic Multidecadal Oscillation (AMO) [*Knight et al.*, 2006; *Zhang and Delworth*, 2006], a spatially homogeneous SST pattern in the North Atlantic that fluctuates on multidecadal time scales [*Enfield et al.*, 2001]. The correlation of our NBC transport time series and Atlantic SST resembles the AMO pattern as shown in Figure 6. The opposite sign of SST variability in the North and South Atlantic across the equator has been associated with northward heat transport by the AMOC [*Yang*, 1999; *Vellinga and Wu*, 2004]. *Latif et al.* [2006] argued that the SST difference between the North and South Atlantic can be used to infer

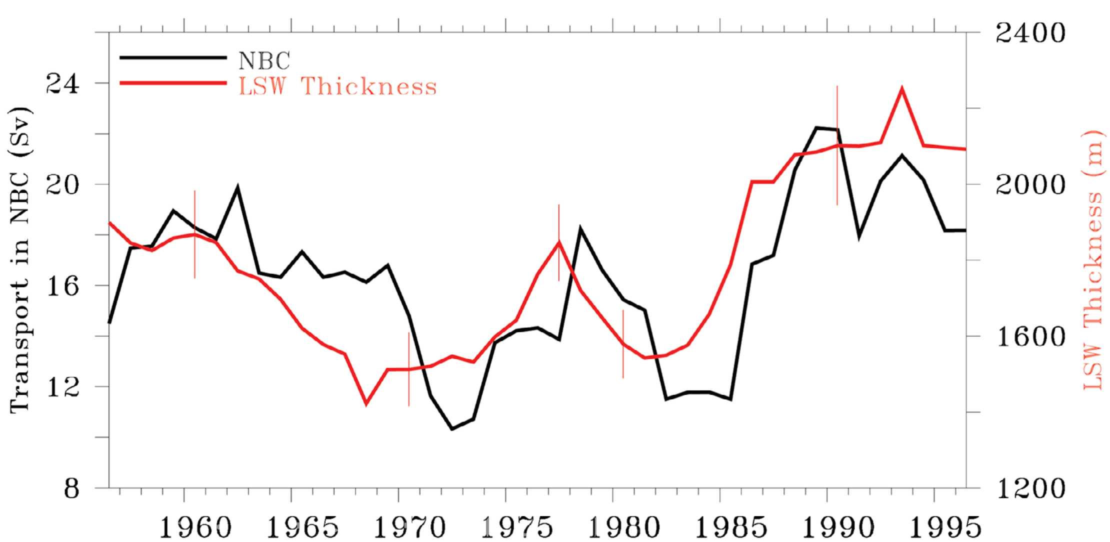

Figure 5. The NBC transport time series compared to the LSW thickness between 34.62 and 34.72 $\sigma_{1.5}$ density surfaces in the Labrador Sea as defined by *Curry et al.* [1998].

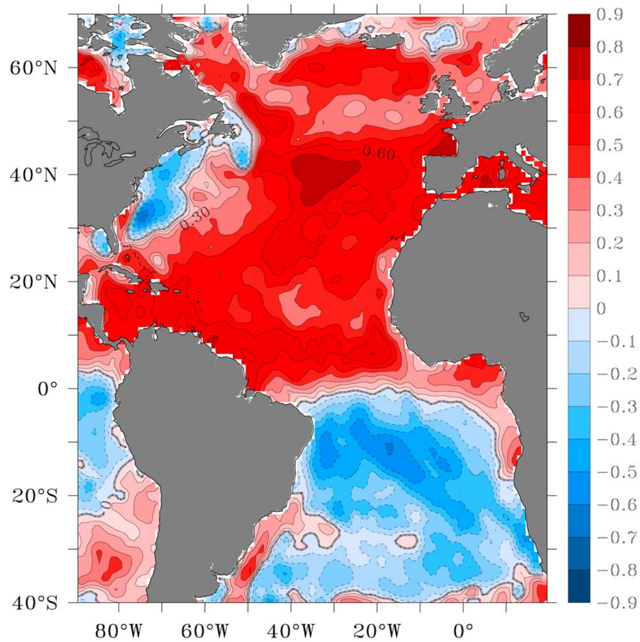

Figure 6. Correlation map of the NBC and detrended SST, showing the homogeneous AMO pattern in the North Atlantic. SST observations were obtained from the Hadley Centre data set (HadISST) at http://badc.nerc.ac.uk/data/hadisst/. The NBC transport is correlated with the AMO index at 0.73 at 0 lag, which is significant at greater than 95% confidence.

AMOC variations in the past. Our transport time series of NBC is significantly correlated with the AMO index [*Knight et al.*, 2006] at zero lag (0.73), suggesting a direct connection with the AMOC. The exact mechanism explaining the basin-scale AMO SST pattern and its relation with the AMOC is not clear. Sensitivity experiments using the tropical and extratropical part of the observed AMO SST pattern to force atmospheric general circulation models, suggest a dominant influence of the tropical Atlantic [*Sutton and Hodson*, 2005, 2007; *Kushnir et al.*, 2010], where the SST pattern could be set by the AMOC or NBC variability [*Yang*, 1999; *Vellinga and Wu*, 2004]. The proposed mechanism involves teleconnections with the northern North Atlantic that could quickly affect SST through changing surface heat fluxes. Another possible explanation is that the basin-scale SST anomalies could be a direct response to changes in the subpolar North Atlantic associated with the AMOC. The fast equatorward progression of the midlatitude SST anomalies can be dominated by an atmosphere-surface ocean mechanism involving the wind-evaporation-SST feedbacks and an anomalous north-south migration of Inter-Tropical Convergence Zone, which are responsible for the asymmetry of SST anomalies across the equator [*Xie*, 1999; *Chiang and Bitz*, 2005; *Cheng et al.*, 2007; *Chiang et al.*, 2008; *Chang et al.*, 2008]. However further work is required to clarify the respective role of the tropics and the influence of high-latitude forcing.

4. The NBC and AMOC in Climate Model GFDL's CM2.1

[13] The uncertainties of our estimation of NBC transport with the mean error of ±3.4 Sv (including possible seasonal aliasing) are large compared to the transport signal with the standard deviation of ±3.1 Sv. But the transport values in the 1970s and 1980s are significantly lower than those in the early 1960s and 1990s, and the timing of the NBC variation fits well with physical models that predict the NBC/AMOC's response to the LSW variability and its effect on the North Atlantic SST. To further confirm the relationship between the NBC and the AMOC, we analyze results of a state-of-the-art climate model, the GFDL's CM2.1 global coupled model [*Delworth et al.*, 2006]. The model simulation analyzed here is a 700 year long segment of a 3000 year long control run in which the concentration of greenhouse gases is fixed at the preindustrial level. The 700 year segment corresponds to that used by *Msadek et al.* [2010] study on the AMOC predictability. Here we used the same data for consistency and ease of presentation. Looking at a longer segment of the simulation would give

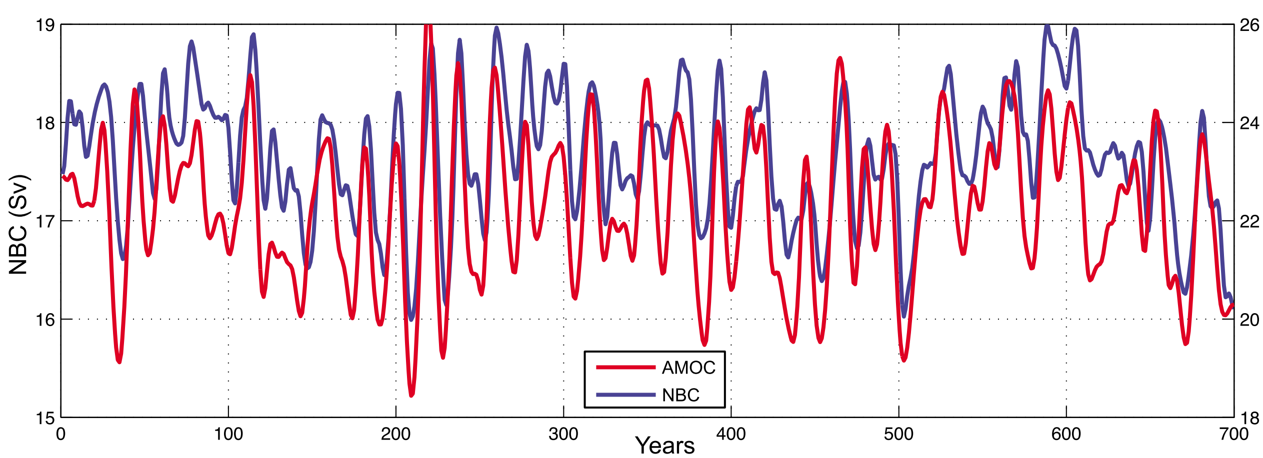

Figure 7. Transport time series of the NBC and the AMOC low-pass filtered at 10 years for a 700 year long segment of the GFDL's CM2.1 control simulation.

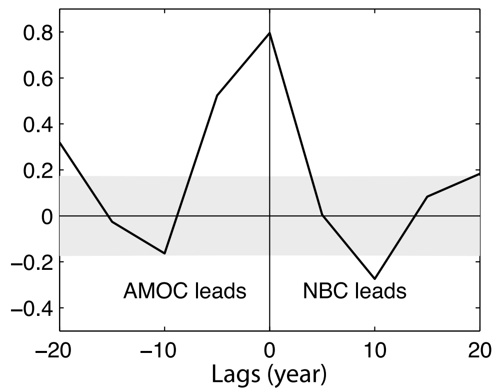

Figure 8. Lagged correlation between the NBC and AMOC transport time series of Figure 7. The grey shading indicates the 95% significance level.

similar results. In the model, the AMOC transport can be unambiguously defined, as well as the relationship between AMOC and NBC.

[14] Following previous studies, the AMOC transport is defined each year as the maximum value of the mean stream function in the North Atlantic. As the maximum of the mean AMOC is located around 40°N in the GFDL's CM2.1 model, using that fixed latitude to define the AMOC index yields to similar results. The NBC transport is calculated in the upper 1200 m of the western boundary current at 6°S in the model. Figure 7 shows the transport time series of the NBC and AMOC over a 700 year segment of the 3000 year run. The correlation of the NBC and AMOC transport reaches its maximum value of 0.8 at zero lag (Figure 8). The model Labrador Sea deep convection index is defined by the maximum winter mixed layer depth averaged over the region where the winter standard deviation exceeds 300 m. In the model, Labrador Sea deep convection leads the AMOC by 6–7 years (Figure 9), with a maximum correlation of 0.5. The longer lag time compared to 2–3 years suggested in Figure 5 is consistent with [*Getzlaff et al.*, 2005] results for coarse resolution forced ocean models although further work

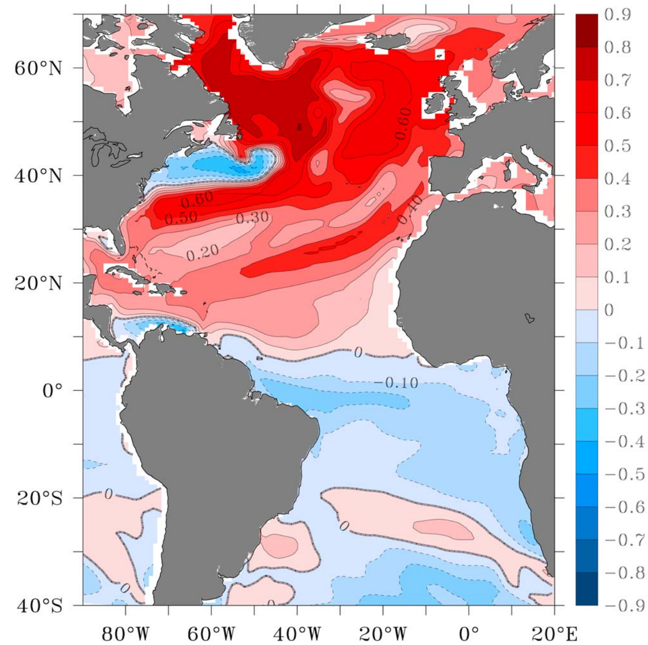

Figure 10. Correlation map of the low-pass filtered SST anomalies and the NBC transport time series in the GFDL's CM2.1 control simulation. As in the observations (Figure 6) the homogeneous North Atlantic pattern closely resembles the model AMO and the correlation between the NBC and AMO time series equals 0.64 at lag 0, which exceeds the 95% significance level.

is required to assess the responsible mechanisms. *Zhang* [2010] attributed the longer lag in the GFDL coupled model to the anomalous gyre circulation in the western subtropical and subpolar Atlantic. The modeled SST associated with the NBC and AMOC transport at zero lag are identical (only the correlation with the NBC is shown in Figure 10) and closely resembles the observed and modeled AMO pattern. The correlation between the NBC and the AMO time series in the

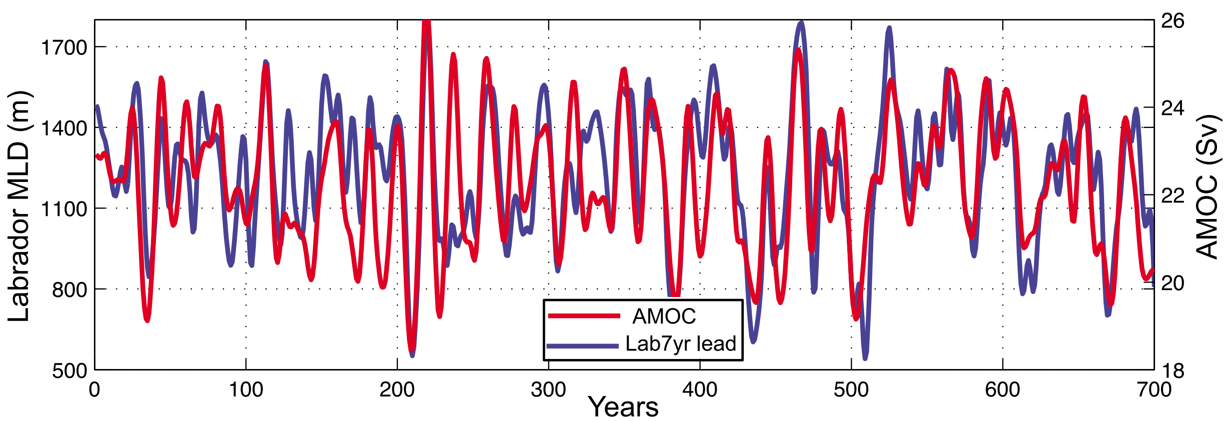

Figure 9. Time series of the AMOC transport and the Labrador Sea deep convection index low-pass filtered at 10 years for a 700 year long segment of the GFDL's CM2.1 control simulation. Deep water formation in the Labrador Sea is defined in the region where the standard deviation of the winter mixed layer depth exceeds 300 m, and the Labrador deep convection index is the winter mixed layer depth averaged over this area. The index is shifted by 7 years, showing its lead to the AMOC transport.

model equals 0.64 at lag 0, which exceeds the 95% significance level. Hence, the modeled relationship between the NBC, AMOC, Labrador Sea deep convection, and SST corroborates that suggested by our observational analysis.

5. Summary and Discussion

[15] Our observed multidecadal NBC transport signal is only marginally significant because of limited data coverage, but the weakening of the NBC in the 1970s and 1980s compared to the high transports in the early 1960s and 1990s are well above the noise level even when possible seasonal aliasing is considered. In addition the observed transport time series of the upper 300 m in the NBC is consistent with a forced eddy permitting model simulation in both amplitude and phase [*Hüttl and Böning*, 2006]. Caution, however, needs to be exercised when interpreting the timing of our observed NBC variability due to data limitations. Nevertheless, our observed relationship of NBC and LSW thickness supports earlier results of idealized model experiments on the response of AMOC/NBC to Labrador Sea deep convection through boundary waves [*Yang*, 1999; *Johnson and Marshall*, 2004; *Getzlaff et al.*, 2005]. The high correlation with the AMO, that has been widely associated with the AMOC, also supports the connection of the NBC with AMOC. Though model simulations have shown variations in the basin-scale structure of the AMOC in the North Atlantic Subtropical gyre on synoptic to interannual time scales [*Bingham et al.*, 2007; *Cunningham et al.*, 2007], the modeled AMOC is coherent across the North and South Atlantic on decadal and longer time scales [*Vellinga and Wu*, 2004; *Msadek and Frankignoul*, 2009]. Theory and numerical models suggest that the low-latitude tropical South Atlantic is well suited for detection of low-frequency multidecadal variability in the AMOC, because the equator acts as a low-pass filter of the high-frequency variability forced in the North Atlantic [*Johnson and Marshall*, 2004]. Given that there is a direct connection between the AMOC and observed AMO variability, our observational analysis suggests that multidecadal variability of NBC at 6°S, where interior currents are predominately zonal, can serve as an indicator of low-frequency variability in the AMOC. This suggestive observational conclusion is supported by the excellent correlation between the NBC and AMOC in the multicentury simulation of GFDL's CM2.1 coupled climate model, though a more thorough analysis of the model is needed to understand the mechanisms that link NBC decadal variability with the AMOC. In addition to coastal Kelvin waves [*Yang*, 1999; *Johnson and Marshall*, 2004; *Getzlaff et al.*, 2005], other mechanisms such as the horizontal gyre dynamics [*Zhang*, 2010], lower-latitude Rossby wave amplification [*Köhl and Stammer*, 2008], and wind driven cross-equatorial flows [*Lee and Wang*, 2008] may affect the connection between the NBC, the Labrador Sea deep convection, and the AMOC. We will focus on these issues in a future study using the GFDL and other models in the Coupled Model Intercomparison Project [*Meehl et al.*, 2007].

[16] A slowdown of the AMOC has been reported from analysis of 5 hydrographic sections over the past 50 years [*Bryden et al.*, 2005] and, while those results are controversial because of the limited data on which they are based, almost all state-of-the-art climate models project significant slowdown of the AMOC during this century in response to the increased greenhouse gas concentrations in the atmosphere [*Meehl et al.*, 2007; *Schmittner et al.*, 2005; *Hu et al.*, 2009]. Our results on the other hand suggest that such an anticipated slowdown has not occurred yet even though global temperatures have been significantly higher since the 1970s. While the AMOC might have been weakened from the 1960s to the early 1970s, it has been strengthening since then to the end of last century as shown in our transport time series. The lack of a weakening trend may be due to an AMOC stabilized by increased northward salinity transport from the warm and saline tropical and subtropical Atlantic [*Curry et al.*, 2003; *Latif et al.*, 2000] and increased meridional density gradient in the North Atlantic [*Wang et al.*, 2010; *Wu et al.*, 2004]. Analyses of subsurface temperature and salinity anomalies in the subtropical and subpolar north Atlantic [*Zhang*, 2008; *Wang et al.*, 2010] also suggest a strengthening of the AMOC from the 1970s to 1990s. Intensified westerly wind and surface heat flux anomalies associated with an upward trend of North Atlantic Oscillation [*Hoerling et al.*, 2001], as well as aerosol effects [*Delworth and Dixon*, 2006], may also have played a role in stabilizing the AMOC. A more in depth assessment of how the AMOC is responding to changing anthropogenic forcing is a critical research challenge, but is beyond the scope of this paper.

[17] **Acknowledgments.** The authors would like to acknowledge the anonymous reviewers for their very helpful comments on an earlier version of the manuscript. This publication was funded by the NOAA's Climate Program Office and the Joint Institute for the Study of the Atmosphere and Ocean (JISAO) under NOAA Cooperative Agreement NA17RJ1232, JISAO publication 1842, and PMEL publication 3659.

References

Balmaseda, M. A., G. C. Smith, K. Haines, D. Anderson, T. N. Palmer, and A. Vidard (2007), Historical reconstruction of the Atlantic meridional overturning circulation from the ECMWF operational ocean reanalysis, *Geophys. Res. Lett.*, *34*, L23615, doi:10.1029/2007GL031645.

Bingham, F., and L. Talley (1991), Estimates of Kuroshio transport using an inverse technique, *Deep Sea Res. Part A*, *38*, suppl. 1, S21–S43.

Bingham, R. J., C. W. Hughes, V. Roussenov, and R. G. Williams (2007), Meridional coherence of the North Atlantic meridional overturning circulation, *Geophys. Res. Lett.*, *34*, L23606, doi:10.1029/2007GL031731.

Boyer, T. P., J. I. Antonov, H. Garcia, D. R. Johnson, R. A. Locarnini, A. V. Mishonov, M. T. Pitcher, O. K. Baranova, and I. Smolyar (2006), *World Ocean Database 2005* [DVDs], *NOAA Atlas NESDIS*, vol. 60, edited by S. Levitus, 190 pp., U.S. Government Printing Office, Washington, D. C.

Bryden, H. L., H. R. Longworth, and S. A. Cunningham (2005), Slowing of the Atlantic meridional overturning circulation at 25°N, *Nature*, *438*, 655–657.

Chang, P., R. Zhang, W. Hazeleger, C. Wen, X. Wan, L. Ji, R. J. Haarsma, W. Breugem, and H. Seidel (2008), Oceanic link between abrupt changes in the North Atlantic Ocean and the African monsoon, *Nat. Geosci.*, *1*, 444–448.

Cheng, W., C. Bitz, and J. C. H. Chiang (2007), Adjustment of the global climate to an abrupt slowdown of the Atlantic meridional overturning circulation, in *Ocean Circulation: Mechanisms and Impacts*, *Geophys. Monogr. Ser.*, vol. 173, edited by A. Schmittner, J. Chiang, and S. Hemming, pp. 295–313, AGU, Washington, D. C.

Chiang, J. C. H., and C. M. Bitz (2005), Influence of high latitude ice cover on the marine intertropical convergence zone, *Clim. Dyn.*, *25*, 477–496.

Chiang, J. C. H., W. Cheng, and C. M. Bitz (2008), Fast teleconnections to the tropical Atlantic sector from Atlantic thermohaline adjustment, *Geophys. Res. Lett.*, *35*, L07704, doi:10.1029/2008GL033292.

Cunningham, S. A., et al. (2007), Temporal variability of the Atlantic meridional overturning circulation at 26.5°N, *Science*, *317*, 935–938.

Curry, R. G. (1996), Hydrobase: A database of hydrographic stations and tools for climatological analysis, *Tech. Rep. WHOI-96-01*, Woods Hole Oceanogr. Inst., Woods Hole, Mass.

Curry, R. G., M. S. McCartney, and T. M. Joyce (1998), Oceanic transport of subpolar climate signals to mid-depth subtropical waters, *Nature*, *391*, 575–577.

Curry, R., B. Dickson, and I. Yashayaev (2003), A change in the freshwater balance of the Atlantic Ocean over the past four decades, *Nature*, *426*, 826–829.

Davis, R. E. (1976), Predictability of sea surface temperature and sea level pressure anomalies over the North Pacific Ocean, *J. Phys. Oceanogr.*, *6*, 249–266.

Delworth, T. L., and K. W. Dixon (2006), Have anthropogenic aerosols delayed a greenhouse gas-induced weakening of the North Atlantic thermohaline circulation?, *Geophys. Res. Lett.*, *33*, L02606, doi:10.1029/2005GL024980.

Delworth, T. L., et al. (2006), GFDL's CM2 global coupled climate models. Part I: Formulation and simulation characteristics, *J. Clim.*, *19*, 643–674.

Enfield, D., A. Mestas-Nunez, and P. Trimble (2001), The Atlantic Multidecadal Oscillation and its relation to rainfall and river flows in the continental US, *Geophys. Res. Lett.*, *28*, 2077–2080.

Getzlaff, J., C. W. Böning, C. Eden, and A. Biastochm (2005), Signal propagation related to the North Atlantic overturning, *Geophys. Res. Lett.*, *32*, L09602, doi:10.1029/2004GL021002.

Hazeleger, W., and S. Drijfhout (2006), Subtropical cells and meridional overturning circulation pathways in the tropical Atlantic, *J. Geophys. Res.*, *111*, C03013, doi:10.1029/2005JC002942.

Hoerling, M. P., J. W. Hurrell, and T. Xu (2001), Tropical origins for recent North Atlantic climate change, *Science*, *292*, 90–92.

Hu, A., G. A. Meehl, W. Han, and J. Yin (2009), Transient response of the MOC and climate to potential melting of the Greenland Ice Sheet in the 21st century, *Geophys. Res. Lett.*, *36*, L10707, doi:10.1029/2009GL037998.

Hüttl, S., and C. W. Böning (2006), Mechanisms of decadal variability in the shallow subtropical-tropical circulation of the Atlantic Ocean: A model study, *J. Geophys. Res.*, *111*, C07011, doi:10.1029/2005JC003414.

Johnson, H. L., and D. P. Marshall (2004), Global teleconnections of meridional overturning circulation anomalies, *J. Phys. Oceanogr.*, *34*, 1702–1722.

Knight, J. R., R. J. Allan, C. K. Folland, M. Vellinga, and M. E. Mann (2005), A signature of persistent natural thermohaline circulation cycles in observed climate, *Geophys. Res. Lett.*, *32*, L20708, doi:10.1029/2005GL024233.

Knight, J. R., C. K. Folland, and A. A. Scaife (2006), Climate impacts of the Atlantic Multidecadal Oscillation, *Geophys. Res. Lett.*, *33*, L17706, doi:10.1029/2006GL026242.

Köhl, A., and D. Stammer (2008), Variability of the meridional overturning in the North Atlantic from the 50-Year GECCO state estimation, *J. Phys. Oceanogr.*, *38*, 1913–1930.

Kushnir, Y., R. Seager, M. Ting, N. Naik, and J. Nakamura (2010), Mechanisms of tropical Atlantic SST influence on North American precipitation variability, *J. Clim.*, *23*, 5610–5628.

Latif, M., E. Roeckner, U. Mikolajewicz, and R. Voss (2000), Tropical stabilization of the thermohaline circulation in a greenhouse warming simulation, *J. Clim.*, *13*, 1809–1813.

Latif, M., C. Böning, J. Willebrand, A. Biastoch, J. Dengg, N. Keenlyside, U. Schweckendiek, and G. Madec (2006), Is the thermohaline circulation changing?, *J. Clim.*, *19*, 4631–4637.

Lee, S., and C. Wang (2008), Tropical Atlantic Decadal Oscillation and its potential impact on the equatorial atmosphere-ocean dynamics: A simple model study, *J. Phys. Oceanogr.*, *38*, 193–212.

Lozier, M. S., W. B. Owens, and R. G. Curry (1995), The climatology of the North Atlantic, *Prog. Oceanogr.*, *36*, 1–44.

Lumpkin, R., and K. Speer (2003), Large-scale vertical and horizontal circulation in the North Atlantic Ocean, *J. Phys. Oceanogr.*, *33*, 1902–1920.

Mariano, A., and O. Brown (1992), Efficient objective analysis of dynamically heterogeneous and nonstationary fields via the parameter matrix, *Deep Sea Res. Part A*, *39*, 1255–1271.

Meehl, G. A., et al. (2007), Global climate projections, in *Climate Change 2007: The Physical Science Basis: Working Group I Contribution to the Fourth Assessment Report of the Intergovernmental Panel on Climate Change*, edited by S. Solomon et al., pp. 747–845, Cambridge Univ. Press, New York.

Msadek, R., and C. Frankignoul (2009), Atlantic multidecadal oceanic variability and its influence on the atmosphere in a climate model, *Clim. Dyn.*, *33*, 45–62.

Msadek, R., K. W. Dixon, T. L. Delworth, and W. Hurlin (2010), Assessing the predictability of the Atlantic meridional overturning circulation and associated fingerprints, *Geophys. Res. Lett.*, *37*, L19608, doi:10.1029/2010GL044517.

Rabe, B., F. A. Schott, and A. Köhl (2008), Mean circulation and variability of the tropical Atlantic during 1952–2001 in the GECCO assimilation fields, *J. Phys. Oceanogr.*, *38*, 177–192.

Roemmich, D., and T. McCallister (1989), Large scale circulation of the North Pacific Ocean, *Prog. Oceanogr.*, *22*, 171–204.

Schmittner, A., M. Latif, and B. Schneider (2005), Model projections of the North Atlantic thermohaline circulation for the 21st century assessed by observations, *Geophys. Res. Lett.*, *32*, L23710, doi:10.1029/2005GL024368.

Schott, F. A., and P. Brandt (2007), Circulation and deep water export of the Subpolar North Atlantic during the 1990s, in *Ocean Circulation Mechanisms and Impacts*, *Geophys. Monogr. Ser.*, vol. 173, edited by A. Schmittner, J. Chiang, and S. Hemming, pp. 91–118, AGU, Washington, D. C.

Schott, F. A., M. Dengler, R. Zantopp, L. Stramma, J. Fischer, and P. Brandt (2005), The shallow and deep western boundary circulation of the South Atlantic at 5°–11°S, *J. Phys. Oceanogr.*, *35*, 2031–2053.

Sutton, R. T., and D. L. R. Hodson (2005), Atlantic ocean forcing of North American and European summer climate, *Science*, *309*, 115–118.

Sutton, R. T., and D. L. R. Hodson (2007), Climate response to basin scale warming and cooling of the North Atlantic Ocean, *J. Clim.*, *20*, 891–907.

Vellinga, M., and P. Wu (2004), Low-latitude freshwater influence on centennial variability of the Atlantic thermohaline circulation, *J. Clim.*, *17*, 4498–4511.

Wang, C., S. Dong, and E. Munoz (2010), Seawater density variations in the North Atlantic and the Atlantic meridional overturning circulation, *Clim. Dyn.*, *34*, 953–968.

Wu, P., R. Wood, and P. Stott (2004), Does the recent freshening trend in the North Atlantic indicate a weakening thermohaline circulation?, *Geophys. Res. Lett.*, *31*, L02301, doi:10.1029/2003GL018584.

Xie, S. P. (1999), A dynamic ocean-atmosphere model of the tropical Atalantic decadal variability, *J. Clim.*, *12*, 64–70.

Yang, J. (1999), A linkage between decadal climate variations in the Labrador Sea and the tropical Atlantic Ocean, *Geophys. Res. Lett.*, *26*, 1023–1026.

Zhang, D., M. J. McPhaden, and W. E. Johns (2003), Observational evidence for flow between the subtropical and tropical Atlantic: The Atlantic subtropical cells, *J. Phys. Oceanogr.*, *33*, 1783–1797.

Zhang, R. (2008), Coherent surface-subsurface fingerprint of the Atlantic meridional overturning circulation, *Geophys. Res. Lett.*, *35*, L20705, doi:10.1029/2008GL035463.

Zhang, R. (2010), Latitudinal dependence of Atlantic meridional overturning circulation (AMOC) variations, *Geophys. Res. Lett.*, *37*, L16703, doi:10.1029/2010GL044474.

Zhang, R., and T. L. Delworth (2006), Impact of Atlantic Multidecadal Oscillations on India/Sahel rainfall and Atlantic hurricanes, *Geophys. Res. Lett.*, *33*, L17712, doi:10.1029/2006GL026267.

T. Delworth and R. Msadek, NOAA Geophysical Fluid Dynamics Laboratory, Princeton University Forrestal Campus, 201 Forrestal Rd., Princeton, NJ 08542, USA. (tom.delworth@noaa.gov; rym.msadek@noaa.gov)

M. J. McPhaden and D. Zhang, NOAA Pacific Marine Environmental Laboratory, 7600 Sand Point Way NE, Building 3, Seattle, WA 98115, USA. (michael.j.mcphaden@noaa.gov; dongxiao.zhang@noaa.gov)